Main-Chain Scission of a Charged Fifth-Generation Dendronized Polymer

by **Hao Yu**, **A. Dieter Schlüter***, and **Baozhong Zhang***

Department of Materials, Laboratory of Polymer Chemistry, ETH Zürich, HCI H528, Wolfgang-Pauli-Strasse 10, CH-8093 Zürich
(e-mail: baozhong.zhang@mat.ethz.ch, ADS@mat.ethz.ch)

Dedicated to Professor *Dieter Seebach* on the occasion of his 75th birthday

During divergent synthesis of the next higher-generation dendronized polymer (DP), the fifth-generation DP, PG5, with a number-average degree of polymerization, (*i.e.*, number of monomeric units) P_n, of *ca.* 500 underwent main-chain scission. This happened in the step when its peripheral Boc groups were removed by the treatment with trifluoroacetic acid (TFA), and thus a heavily charged polyelectrolyte formed as an intermediate. Atomic Force Mircoscopy (AFM) analysis of the product after drop-casting onto mica showed a large majority of short deprotected PG5 chains with P_n of *ca.* 40, as well as some smaller features that by MALDI-TOF mass spectrometry and ^{1}H-NMR spectroscopy were assigned to the hypothetical monomer, deprotected MG5. This behavior is compared to a recently reported main-chain scission of a closely related PG5 which, however, resulted in significantly longer fragments. While this difference cannot yet be fully explained, questions are formulated which will guide future research.

Introduction. – Dendronized polymers (DPs) are comb polymers bearing regularly branched dendrons at each main-chain repeat unit [1]. This results in an encapsulation of the polymer chain by the surrounding dendrons, which causes unique features of DP. These include a rigidified backbone [2], a tuneable main chain thickness that is responsive to external stimuli [3], and a large number of 'surface' functional groups resulting in a variety of biological and other applications[1]). If the generation and thus the size of the pendent dendrons increase, steric repulsion between the dendrons also increases. Theoretically, this can go so far until there is no enough space anymore to accommodate all the dendrons around the backbone. This packing limit will result in structure defects if the growth of dendrons is continued [5]. Regarding the DPs our group is currently working on (*Fig. 1*), the maximum generation was estimated as $g = 6$ [5]. Such large substituents, being densely grafted at small distances, may induce strain in the main chain, which will weaken the DPs backbone towards chain scission upon exposure to external forces. This strain may further be enhanced by *Coulombic* repulsion in DPs that carry charged functional groups in the dendrons' periphery, as is commonly encountered, *e.g.*, during divergent DP synthesis [6]. Previously, we noted the unintentional main chain scission of a fifth generation DP, $PG5_{1000}$ (subscript denotes average degree of polymerization (number of monameric untis), P_n), during the acidic deprotection of its countless (*tert*-butoxy)carbonyl (Boc)-protected amines.

[1]) For biological applications of DPs, see [4a–c]; for other selected applications, see [4d–j].

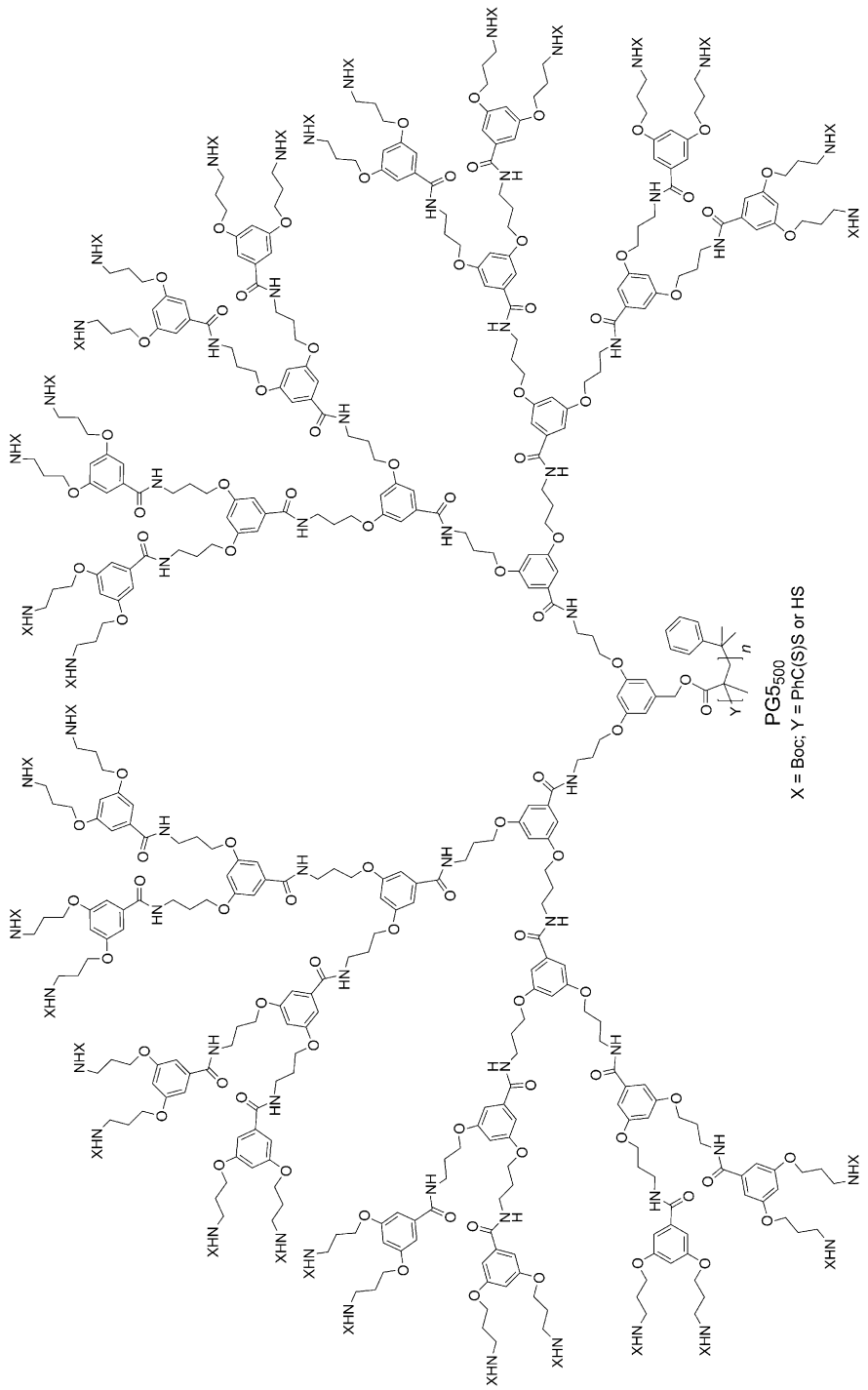

Fig. 1. *Chemical structure of $PG5_{500}$ synthesized according to a RAFT protocol.* The polymers initially carry one benzodithioate end group per chain which subsequently, to a large degree, is converted into thiol, as suggested by the end group analysis by ^{1}H-NMR spectroscopy [6].

This deprotection was intended to first furnish *de*-$PG5_{1000}$ and then $PG6_{1000}$ in the follow-up dendronization step (prefix *de* for 'deprotected') [6]. The chain length of the obtained PG6, however, was much shorter than expected and, on top of this, depended on the stirring speed during deprotection [6]. It was thus assumed that some of the backbone C–C σ bonds were cleaved by mechanical shear force during stirring.

Herein, we report on what happens during the attempted acidic deprotection of another PG5, $PG5_{500}$, which differs from that mentioned above by its shorter chain length (P_n 500 instead of 1000) and particularly the mode of synthesis. It was not synthesized according to a free-radical polymerization (FRP) as $PG5_{1000}$ but rather by a reversible addition fragmentation chain transfer (RAFT) [7] protocol. This ought to help shedding somewhat more light onto the issue of main chain scission. The investigation involves atomic force microscopy (AFM) contour length, gel permeation chromography (GPC), NMR-spectroscopical and mass-spectrometrical analyses of the products. It is further substantiated by the use of a PG5 with short main chain, $PG5_{40}$ [6] for comparison purposes. As will be seen, the matter is rather complex, and the collected mosaic stones are not yet sufficient to give a comprehensive picture of what happens during main chain scission of DP at the fifth generation, but led us to address some unexplored issues which serve as a guideline for future research.

Experimental. – DPs of generation 3–5 (PG3–PG5) were synthesized by the 'attach-to' or divergent method starting from the first generation DP (PG1, P_n *ca.* 500 or 40), prepared by RAFT polymerization using RAFT agent **1**; see the *Scheme*). The synthetic details were published in [6]. The structure perfection of all the synthesized DPs is $>99\%$, as quantified by the well-established UV-labeling method [8].

^{1}H-NMR Recordings were performed on *Bruker AV 300* (300 MHz), and *500* (500 MHz) spectrometers at r.t. Chemical shifts are reported as δ values (ppm). Gel permeation chromatography (GPC) was carried out with a PL-GPC 220 instrument with a *2 × PL-Gel Mix-B LS* column set (2 × 30 cm) equipped with refractive-index (RI), viscometry, and light-scattering (LS; 15° angle) detectors, and LiBr (1 g/l) in DMF as eluent at 45°. Universal calibration was performed with poly(methyl methacrylate) standards in the Mp range of 2680–1500000 (*Polymer Laboratories Ltd.*, UK). AFM was performed with a *Nanoscope IIIa* multimode scanning probe microscope (*Digital Instruments*, San Diego, CA) in the tapping mode with an *E* scanner (scan range 10 μm × 10 μm) at ambient conditions. *Olympus* silicon *OMCL-AC160TS* cantilevers (*Atomic Force F&E GmbH*, D-Mannheim) with a resonance frequency in the range of 200–400 kHz (typically *ca.* 300 kHz) and a spring constant *ca.* 42 N/m was used. The specimen for AFM were prepared by drop-casting the polymer soln. (3 to 4 mg/l in CH_2Cl_2, $CHCl_3$, or MeOH) onto freshly cleaved mica (*PLANO W. Plannet GmbH*, D-Wetzlar). Typical measurements were performed with amplitude set point ranging from 0.5 to 2.0 V and drive amplitude ranging from 5 to 90 mV. No deconvolution was performed. MALDI-TOF Mass spectrometry was performed by an *IonSpec Ultra* instrument, using 2,5-dihydroxybenzoic acid (DHB), 2-{(2*E*)-[4-(*tert*-butyl)phenyl]-2-methylprop-2-enylidene}malononitrile (DCTB), or 3-hydroxypyridine-2-carboxylic acid (3-HPA) as the matrix.

Results and Discussion. – The divergent build-up of DP is commonly performed by starting from a first-generation DP, PG1, of a particular main chain length which is then first deprotected to *de*-PG1, before the next generation is added by attaching the active ester dendron reagent DG1 onto *de*-PG1 to afford PG2 (*Scheme*, *a*) [9]. This new DP ideally has the same chain length and chain-length distribution as the previous generation. This sequence can then be carried through without unexpected encounters up to PG5, whereby the starting DP is commonly synthesized by FRP. Upon attempted

Scheme. a) *Divergent Synthesis of DPs with ever Increasing Generations.* b) *Synthesis of $PG1_{500}$ from Monomer MG1 Using RAFT Agent* **1**. Boc = (*tert*-Butoxy)carbonyl; AIBN = azoisobutyronitrile.

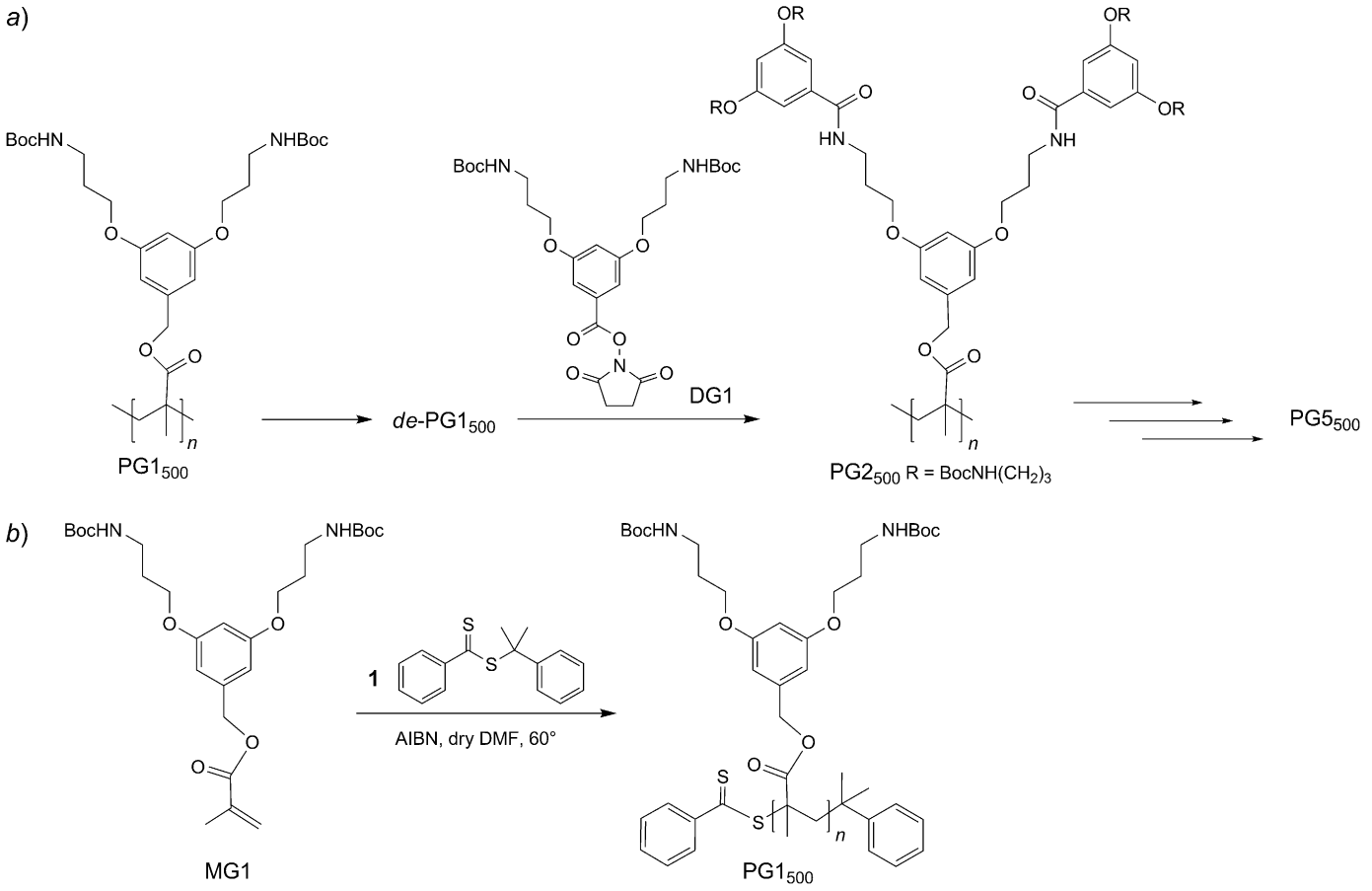

continuation of this sequence to PG6, however, indications for main-chain scissions were observed [6]. Because of the obvious detrimental impact such encounters have on the accessibility of this and even higher generation DP, we set out to explore this matter in more detail.

Termination by recombination in FRP results in C–C bonds in the main chain that are more highly substituted than the others and, therefore, weaker[2]). To avoid complications through the presence of such potential predetermined breaking points, we synthesized a $PG1_{500}$ according to the RAFT protocol [7], where recombination is largely suppressed. Another reason to apply RAFT polymerization was to achieve a narrower molar-mass distribution than in FRP products, which should be beneficial whenever chain scission is to be detected by AFM contour-length (L_{cont}) analysis. Thus, the starting polymer was obtained as shown in *Scheme*, *b*, and then fed into the sequence in *a* to finally give $PG5_{500}$. *Fig. 2*, *a*, shows a TM-AFM height image of this polymer to confirm its regular structure and to assess L_{cont}. Visual inspection gave L_{cont} of *ca.* 100 nm. $PG5_{500}$ was then subjected to the commonly applied deprotection

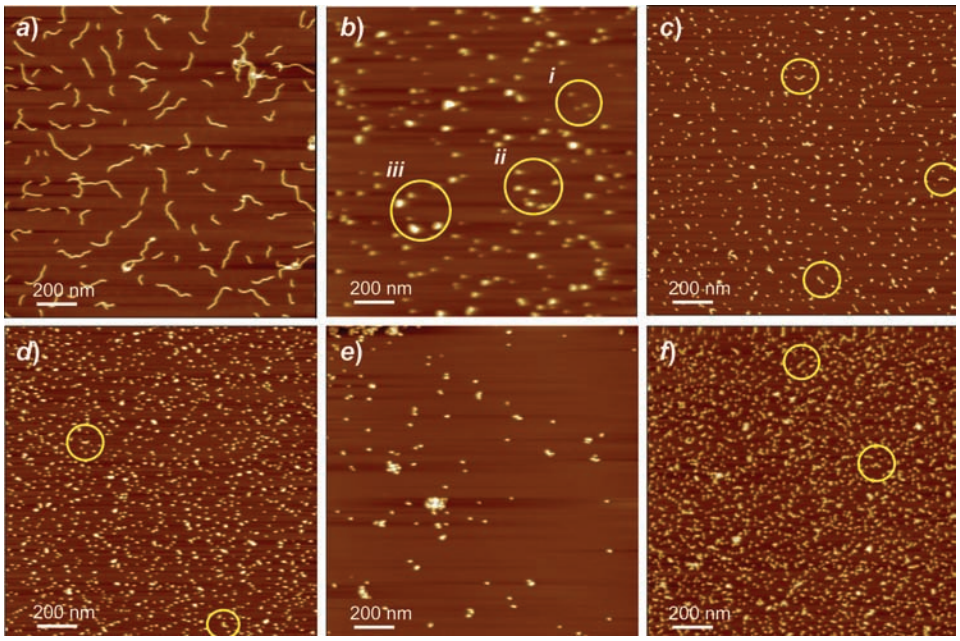

Fig. 2. *AFM Height images of* a) $PG5_{500}$, b) de-$PG5_{500}$, c) $PG6_{500}$, d) $PG5_{40}$, e) de-$PG5_{40}$, *and* f) $PG6_{40}$. Freeze-dried samples were dissolved in CH_2Cl_2 (*a*, *c*, *d*, and *f*) and MeOH (*b* and *e*) at *ca.* 1 mg/l and drop-cast on mica prior to AFM measurements. The circled areas in *b* indicate *i*) 'small' dots with h_{app} of *ca.* 1.2–1.5 nm, *ii*) 'medium' dots with h_{app} of *ca.* 2.0–2.5 nm, and *iii*) 'big' dots with h_{app} of *ca.* 3.0–3.8 nm. The circled areas in *c*, *d*, and *f* indicate short linear chains. *Note:* The height scales of the panels are not normalized in order to obtain good contrast; therefore, features with similar colors in different images may nevertheless differ in their heights. Also, the images were recorded with different tips because of which a direct shape comparison is not possible.

---

[2]) For example, see [10].

conditions (neat TFA, $-10°$, 12 h), followed by MeOH quenching and solvent evaporation ($3\times$). The residue was dissolved in H_2O and freeze-dried to give a product in *ca.* 100% yield, which was assumed to be *de*-$PG5_{500}$.

The product was dissolved in MeOH at *ca.* 1 mg/l and drop-cast onto mica for AFM imaging (*Fig. 2,b*). Obviously, the polymer appears as only small pieces, and we, therefore, refer to this DP as *de*-$PG5_{\cdot 500\cdot}$. The AFM image in *Fig. 2,b*, was recorded at *ca.* 30 min after drop-casting, and the same specimen was imaged again using the same parameters after 12 h, and the result was the same (image not shown). This excludes the concern regarding adsorption-induced chain scission [11]. This view was confirmed by GPC, which showed a decrease of chain length without the chains having ever been exposed to adsorption forces. Because the resolution of charged DP in AFM imaging tends to be unsatisfactory, the *de*-$PG5_{\cdot 500\cdot}$ sample was further converted into its neutral higher-generation analog $PG6_{\cdot 500\cdot}$ (*Scheme,a*). This material was drop-cast from CH_2Cl_2 solution onto mica for AFM analysis (*Fig. 2,c*). To assess the chain length of $PG6_{\cdot 500\cdot}$, the previously synthesized short chain DPs, $PG5_{40}$, *de*-$PG6_{40}$, and $PG6_{40}$ [6], were also imaged (*Fig. 2,d–f*). While a quantitative comparison of the two series of DPs was not performed, the similarities between *de*-$PG5_{\cdot 500\cdot}$ and the authentic *de*-$PG5_{40}$, as well as between $PG6_{\cdot 500\cdot}$ and the authentic $PG6_{40}$ are striking. It seems that the scission process in solution has resulted in chain fragments that, to a large degree, consist of *ca.* 40 repeat units. This important point was substantiated by GPC analysis of $PG6_{\cdot 500\cdot}$ and $PG6_{40}$ which both gave virtually identical elution times (*Fig. 3*).

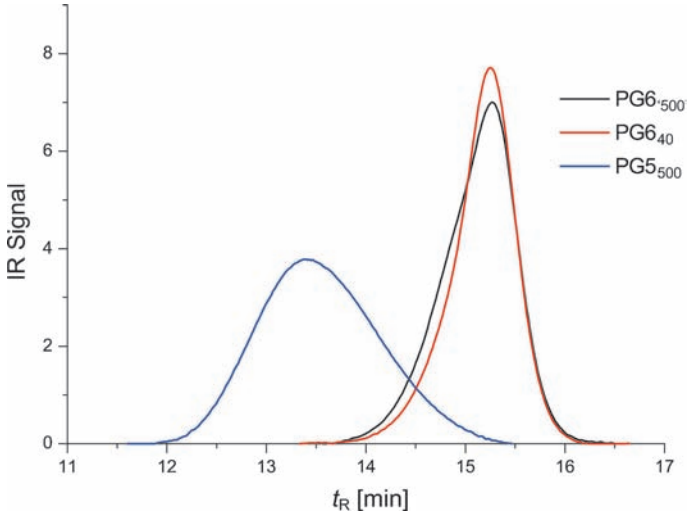

Fig. 3. *GPC Elution curves of* $PG6_{\cdot 500\cdot}$ *and* $PG6_{40}$ *in comparison with* $PG5_{500}$

The AFM images contain more valuable information which is based on the apparent heights (h_{app}). *Fig. 2,b*, contains more or less dot-like features that have different heights (ranging from 1.2 to 3.8 nm) and diameters. A few examples were circled (*i–iii*) according to their h_{app} values: *i*) h_{app} 1.2–1.5 nm, *ii*) h_{app} 2.0–2.5 nm, and *iii*) h_{app} 3.0–3.8 nm. While the nature of the medium features can at present only be speculated about, the large features are reminiscent of authentic *de*-$PG5_{40}$ for which

h_{app} in the range of 2.8–4.0 nm was measured (though aggregates cannot be excluded). They were, therefore, tentatively assigned to fragments of the initial $PG5_{500}$ sample that contain *ca.* 40 repeat units. The smallest features that have h_{app} values of slightly more than 1 nm are considered particularly interesting, because such small h_{app} values cannot be reasonably brought into connection with the DPs discussed here anymore, despite the substantial uncertainty associated with TM-AFM height determinations [12]. In *Fig. 2*, *c*, *d*, and *f*, among the major dot-like features, short linear chains were also observed, which were *ca.* 30–50 nm in length[3]). Thus, any mechanistic proposals have to take into consideration that not only fragmentation occurs but that also short chains are in the product.

Depolymerization is a common phenomenon in polymer chemistry [13]. If there is a mechanism available for chain-end activation, polymer chains will unzip back to release monomers when the temperature is raised beyond the ceiling temperature, T_c. For vinyl polymers of daily use, T_c tends to be so high that depolymerization is not commonly observed. As the steric load on polymers increases by the introduction of sterically increasingly demanding substituents, however, T_c decreases, which, in other words, means that polymer chains undergo depolymerization already at lower temperature to release the steric strain. For example, *Yamada et al.* reported a T_c value of 146° for polyphenylmethacrylate, while T_c is reduced to 33°, if two bulky i-Pr groups are introduced at the *ortho*-positions of the phenyl group [14]. By introducing even larger 2,6-diisobutyl groups, T_c of $-46°$ was calculated by extrapolation. T_c Values for DPs have never been reported. Given the finding that *de*-$PG5_{\cdot 500}$ is similar to these polymethacrylates and strain is caused by both steric and *Coulombic* repulsion, we figured that, for this DP, T_c[4]) may be in or even below the temperature range in which the deprotection was carried out ($-10°$ to room temperature). We, therefore, investigated the sample *de*-$PG5_{\cdot 500}$ more closely to find evidence for the occurence of depolymerization product which would be the so far hypothetical macromonomer *de*-MG5. The sample was subjected to MALDI-TOF mass spectrometry and ^{1}H-NMR spectroscopy, the results of which are shown in *Fig. 4*.

Both spectra show that macromonomer *de*-MG5 is in fact present in the product. Not only does the mass spectrum exhibit the corresponding high-resolution molecular-ion peak at *m*/*z* 7851.58, but also the ^{1}H-NMR spectra at room temperature and at 80° show the signature of an acrylate repeat unit with the olefinic signals at δ 5.8 and 6.0 ppm[5]). These analytical methods provide even more valuable informations. The mass spectrum shows peaks at lower *m*/*z* values which were assigned to the same macromonomer *de*-MG5 but with structural defects caused by one missing branch unit (*m*/*z* 7591.02) and three missing branch units (*m*/*z* 7098.84) of the overall 31 branch units of the perfect macromonomer. While these defects may allow for an independent

---

[3]) The AFM apparent heights of these short chains are 7.3–7.8 nm (in *c*), 3.6–4.2 nm (in *d*), and 4.3–5.3 nm (in *f*). Note that these images are recorded under completely different conditions, the seemingly large value of the apparent height in *Fig. 2*, *c*, compared to that in *Fig. 2*, *f*, does not reflect the actual difference between $PG6_{\cdot 500}$ and $PG6_{40}$. By inspection of more AFM images of $PG6_{\cdot 500}$ and $PG6_{40}$, it is noted that their apparent heights are effectively the same.

[4]) Ceiling temperature for the polymerization of charged monomers are rarely reported, see [15].

[5]) The possibility of backbiting, followed by β scission, to yield alkene terminated DP, can be ruled out by the AFM result; see [16].

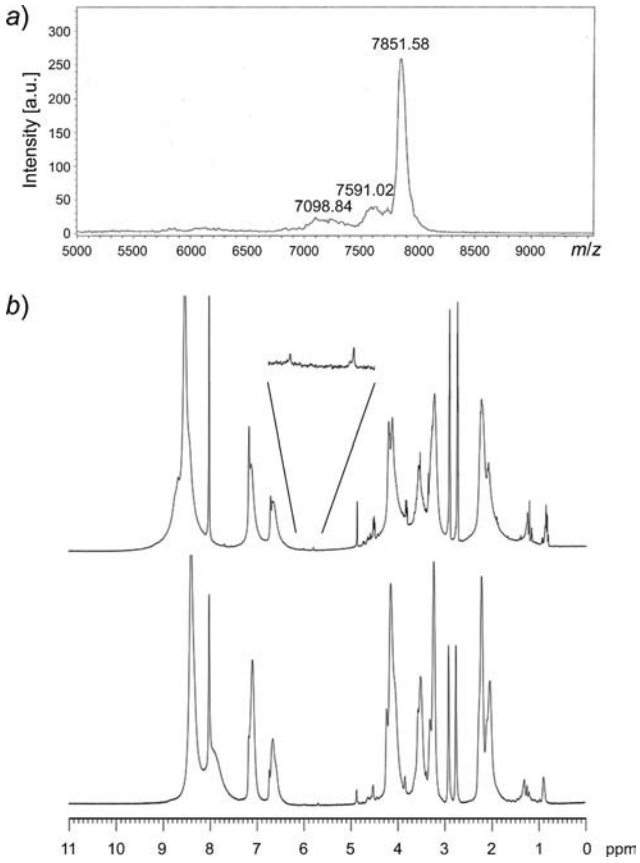

Fig. 4. a) *Analysis of the attempted deprotection of* $PG5_{500}$ *resulting in* de-$PG5_{500}$, *based on high-resolution MALDI-TOF mass spectrum.* b) ^{1}*H-NMR Spectra at 20°* (top) *and 80°* (bottom) *in* (D_6)*DMSO.* The signals at *m*/*z* 7591.02 and 7098.84 in *a*) stand for the macromonomer *de*-MG5 with imperfectly branched structures.

quantification of the (very high) structural integrity of DP [6], they have no bearing on the aspect of depolymerization and are, therefore, not further considered here. Further, there are no signs of either lower (5000–7000) or higher masses (> 8000). The former excludes the possibility of a cleavage within the dendritic structures, which would have produced smaller fragments. The latter is in line with earlier unsuccessful attempts to get DP to fly in the mass spectrometer under MALDI conditions. Thus, the oligomers that may exist in the analyzed sample, as deduced from the AFM analysis shown in *Fig. 2*, do not appear in the mass spectrum. They do, however, show in the NMR spectra (*Fig. 4*, *b*; see the inset with the expanded olefinic region). Because of the charged nature and large size of the macromolecules investigated by NMR, even the higher-temperature spectrum is not perfectly resolved rendering integration unreliable. According to a rough estimation, the macromonomer fraction in the oligomer is on the order of just a few percent. This explains why there is no indication of MG6 in the GPC

elution curves in *Fig. 3*[6]). Based on this evidence, we tentatively assign the dot-like features in the AFM image of *Fig. 2, b*, to mainly a mixture of DP oligomers that are short enough to accommodate their dendrons basically on the substrate, as well as macromonomer *de*-MG5. While the fraction of the latter species in the AFM image is assessed to be in the range of 10–20%, given the huge mass difference between macromonomer and short chains with P_n of *ca.* 40, the corresponding mass fraction will be in the estimated range of a few percent. According to this analysis, *de*-$PG5_{\cdot 500 \cdot}$ contains mainly two different structures: a small amount of macromonomer and a large amount of oligomeric DP with P_n of *ca.* 40, which is sufficiently long to create sizeable height. It is also noted that, in the AFM images of $PG6_{\cdot 500 \cdot}$ and $PG6_{40}$ (*Fig. 2, d* and *f*), few longer linear chains (*ca.* 40–80 nm) are also present, which requires explanation.

The aspect of depolymerization/chain scission was qualitatively investigated further aiming to establish that T_c for *de*-$PG5_{500}$ is below room temperature and thus in a range relevant to the deprotection conditions applied. For this purpose, the lower generation congeners, *de*-$PG3_{500}$ and *de*-$PG4_{500}$, were treated by neat CF_3COOH (TFA) at 70° for 72 h. From previous work, it was known that these charged DPs are stable under the common deprotection conditions. However, under these now more forcing conditions we assumed that even these lower-generation DPs would suffer the same fate that *de*-$PG5_{\cdot 500 \cdot}$ already suffers at lower temperature. As shown by AFM imaging, while *de*-$PG3_{500}$ remained unchanged, *de*-$PG4_{500}$ in fact underwent substantial main-chain scission (*Fig. 5*). Thus, the qualitative order of thermal stability is in fact *de*-$PG3_{500}$ > *de*-$PG4_{500}$ > *de*-$PG5_{500}$, which is inversely related to steric crowding and linear charge density.

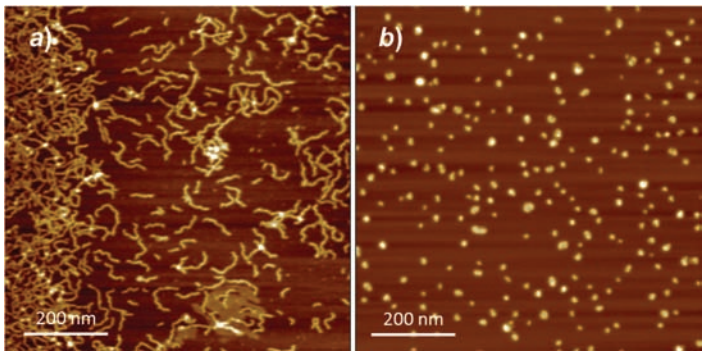

Fig. 5. *AFM Height images of* de-*PG3*$_{500}$ (*a*) *and* de-*PG4*$_{500}$ (*b*)*, after being refluxed in TFA for 72 h, quenched by MeOH, and drop-cast on mica*

After some insight had been already gained into what happens during deprotection of $PG5_{500}$, a final effort was directed towards finding milder deprotection conditions. Particularly, it was tried to subject $PG5_{500}$ to an as short as experimentally possible time to TFA and also to use diluted media. Three conditions were tried: neat TFA for 5 min, solution in DMF for 5 min, and solution in CH_2Cl_2 for 5 min. In all three cases, at least

[6]) Like for *de*-$PG5_{\cdot 500 \cdot}$, any eventually charged MG5 should be converted into neutral MG6 by the reagent DG1.

two features were observed (*Fig. 6*): *i*) a large majority of small dots with h_{app} of *ca.* 3.3 nm and *ii*) a few short polymer chains with h_{app} of *ca.* 3.8–5.2 nm (circled in *Fig. 6, a–c*). The short chains are likely due to the partially deprotected starting material which did not yet suffer full main-chain scission. In CH_2Cl_2, an additional feature was observed. Besides some short polymer chains with h_{app} of *ca.* 3–4 nm, also chains with h_{app} of *ca.* 7 nm were detected (*iii*; circled in *Fig. 6, c*). They are tentatively assigned to nearly unreacted $PG5_{500}$ chains. Note that authentic neutral $PG5_{500}$ also has h_{app} of *ca.* 7 nm, which matches perfectly. Thus, chain scission occurs already early on during deprotection and can only minorly be slowed down under the reaction conditions (CH_2Cl_2). From the finding that, in all cases, some longer chains can still be detected, it is concluded that a certain level of deprotection/charging is required for chain scission to occur, and that, thus, charges actually play a role in weakening the backbone.

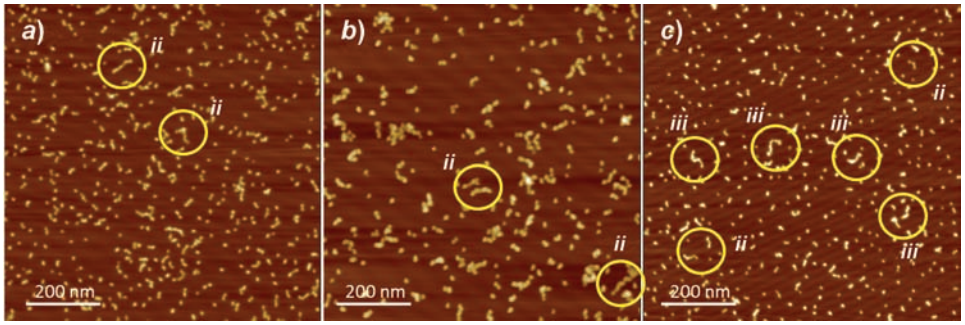

Fig. 6. *AFM Height images of the products of $PG5_{500}$ deprotection under milder conditions such as after 5 min at 0° in* a) *neat TFA,* b) *DMF, and* c) CH_2Cl_2. Samples were quenched and immediately drop-cast on mica. Linear polymer chains with h_{app} of *ca.* 3–5.2 nm and h_{app} of *ca.* 7 nm are circled, and marked as *ii* and *iii*, respectively. h_{app} of *ca.* 7 nm only in *c*.

Chain scission of polymers caused by various external stimuli has been known for decades[7]). Stimuli can be macroscopically applied mechanical forces, flow or shear forces [18], and adsorption forces [11], as well as forces acting during repeated freeze-thaw [19], ultrasound [20], or heat [21] application. Theory has also provided insights into such scission events, whereby recent publications on structurally related bottle-brush polymers are particularly relevant [22]. Among these external stimuli, shear forces during stirring of the reaction solution seem relevant with the previously reported chain scission during deprotection of FRP-$PG5_{1000}$ [6]. This is suggested by a dependence of fragment chain length on stirring speed. While, under low stirring speed of 60 rpm, longer chains (*ca.* 300 nm) were observed [23], stirring at 300 rpm resulted in the majority of chain fragments to be < 100 nm[8]). Crowdedness and charges weaken the DP backbone and thus facilitate scission in shear fields. Chain scission is usually assumed to proceed *via* homolytic bond cleavage of main backbone bonds. Surprisingly, the resulting radicals in the $PG5_{1000}$ fragments do not seem to be centers active towards subsequent depolymerization. The observed fragments are still in the range of 100 nm

[7]) For a review on chain scissions due to mechanical and other forces, see [17].

[8]) AFM Images will be published elsewhere; see [6]. The yields for the deprotection reactions are constantly near quantitative, excluding the possibility of selective chain adsorption on the glassware.

and more! According to the above T_c considerations, they should otherwise initiate depolymerization, until the remaining strain in the DP fragments is liberated. This should be the case when end effects (conformational relaxations) start to dominate the entire DP.

Chain scission of the RAFT-$PG5_{500}$ presented in this publication has a few characteristics that seem to be incompatible with the above: *1*) Fragmentation seems to be independent of shear fields. Under the same conditions where FRP-$PG5_{1000}$ furnishes fragments with average length of 300 nm, RAFT-$PG5_{500}$ furnishes the short fragments discussed above. Stirring speed has no detectable impact on the latter. *2*) Small amounts of monomeric species *de*-MG5 are obtained. *3*) Short linear chains (*ca.* 50–80 nm) are always present in small quantity. Before a full understanding of these differences can be achieved, a couple of questions need to be answered. They include: *a*) What is the activation mechanism for depolymerization? *b*) Can macromonomers, despite steric and charge repulsion, add to radical chain ends? *c*) Can main-chain fragments with radicals at both termini recombine? *d*) Why does FRP-$PG5_{1000}$ cleave into fragments that are still hundreds of nm long without subsequent depolymerization? *e*) Can one differentiate between steric and charge contributions to strain exerted to the backbone?

In summary, $PG5_{500}$ with a RAFT backbone suffers main-chain scission into short fragments which likely is a result of a combination of shear forces, steric strain, and *Coulombic* strain acting on the chains. The length range of these fragments suggests that chain-end relaxation effects play a role in the fragmentation process. The mechanism seems to contain a component of depolymerization.

This work was financially supported by the *Swiss National Science Foundation* (NRP 62 '*Smart Materials*'), which is gratefully acknowledged. We thank Profs. *N. D. Spencer* and *M. Textor*, ETHZ, for access to the AFM instruments.

REFERENCES

[1] A. D. Schlüter, *Top. Curr. Chem.* **1998**, *197*, 165; H. Frey, *Angew. Chem., Int. Ed.* **1998**, *37*, 2193; A. D. Schlüter, J. P. Rabe, *Angew. Chem., Int. Ed.* **2000**, *39*, 864; A. Zhang, L. Shu, Z. Bo, A. D. Schlüter, *Macromol. Chem. Phys.* **2003**, *204*, 328; A. D. Schlüter, *C. R. Chim.* **2003**, *6*, 843; K. Ishizu, K. Tsubaki, A. Mori, S. Uchida, *Prog. Polym. Sci.* **2003**, *28*, 27; A. D. Schlüter, *Top. Curr. Chem.* **2005**, *245*, 151; H. Frauenrath, *Prog. Polym. Sci.* **2005**, *30*, 325; A. Zhang, J. Sakamoto, A. D. Schlüter, *Chimia* **2008**, *62*, 776; B. M. Rosen, C. J. Wilson, D. A.Wilson, M. Peterca, M. R. Imam, V. Percec, *Chem. Rev.* **2009**, *109*, 6275; Y. Chen, X. Xiong, *Chem. Commun.* **2010**, *46*, 5049; J. I. Paez, M. Martinelli, V. Brunetti, M. C. Strumia, *Polymers* **2012**, *4*, 355.

[2] B. Zhang, R. Wepf, K. Fischer, M. Schmidt, S. Besse, P. Lindner, B. T. King, R. Sigel, P. Schurtenberger, Y. Talmon, Y. Ding, M. Kröger, A. Halperin, A. D. Schlüter, *Angew. Chem., Int. Ed.* **2011**, *50*, 737.

[3] W. Li, A. Zhang, A. D. Schlüter, *Macromolecules* **2008**, *41*, 43; W. Li, A. Zhang, K. Feldman, P. Walde, A. D. Schlüter, *Macromolecules* **2008**, *41*, 3659; W. Li, A. Zhang, A. D. Schlüter, *Chem. Commun.* **2008**, 5523; I. Popa, B. Zhang, P. Maroni, A. D. Schlüter, M. Borkovec, *Angew. Chem., Int. Ed.* **2010**, *49*, 4250; M. J. N. Junk, W. Li, A. D. Schlüter, G. Wegner, H. W. Spiess, A. Zhang, D. Hinderberger, *Angew. Chem., Int. Ed.* **2010**, *49*, 5683; M. J. N. Junk, W. Li, A. D. Schlüter, G. Wegner, H. W. Spiess, A. Zhang, D. Hinderberger, *Macromol. Chem. Phys.* **2011**, *212*, 1229.

[4] a) C. C. Lee, S. M. Grayson, J. M. J. Fréchet, *J. Polym. Sci., Part A: Polym. Chem.* **2004**, *42*, 3563; b) C. C. Lee, M. Yoshida, J. M. J. Fréchet, E. E. Dy, F. C. Szoka, *Bioconjugate Chem.* **2005**, *16*, 535;

c) P. Laurino, R. Kikkeri, N. Azzouz, P. H. Seeberger, *Nano Lett.* **2011**, *11*, 73; d) P. R. L. Malenfant, J. M. J. Fréchet, *Macromolecules* **2000**, *33*, 3634; e) K. Krishnamoorthy, A. V. Ambade, S. P. Mishra, M. Kanungo, A. Q. Contractor, A. Kumar, *Polymer* **2002**, *43*, 6465; f) Z. Fei, Y. Han, Z. Bo, *J. Polym. Sci., Part A: Polym. Chem.* **2008**, *46*, 4030; g) H. Jin, Y. Xu, Z. Shen, D. Zou, D. Wang, W. Zhang, X. Fan, Q. Zhou, *Macromolecules* **2010**, *43*, 8468; h) W.-Y Lai, J. W. Levell, A. C. Jackson, S.-C. Lo, P. V. Bernhardt, I. D. W. Samuel, P. L. Burn, *Macromolecules* **2010**, *43*, 6986; i) A. Chakrabarti, A. Juilfs, R. Filler, B. K. Mandal, *Solid State Ionics* **2010**, *181*, 982; j) W. Zhang, H. Jin, D. Wang, Z. Chu, Z. Shen, D. Zou, X. Fan, *J. Polym. Sci., Polym. Chem.* **2012**, *50*, 581.

[5] B. Zhang, R. Wepf, M. Kröger, A. Halperin, A. D. Schlüter, *Macromolecules* **2011**, *44*, 6785.

[6] H. Yu, M. Kröger, A. Halperin, B. Zhang, A. D. Schlüter, in preparation.

[7] J. Chiefari, Y. K. Chong, F. Ercole, J. Krstina, J. Jeffery, T. P. T. Le, R. T. A. Mayadunne, G. F. Meijs, C. L. Moad, G. Moad, E. Rizzardo, S. H. Thang, *Macromolecules* **1998**, *31*, 5559; T. P. Le, G. Moad, E. Rizzardo, S. H. Thang, E. I. Du Pont De Nemours and Co., USA, WO 9801478, 1998; *Chem. Abstr.* **1998**, *128*, 115390f; G. Moad, E. Rizzardo, S. H. Thang, *Aust. J. Chem*. **2005**, *58*, 379.

[8] L. J. Shu, I. Gossl, J. P. Rabe, A. D. Schlüter, *Macromol. Chem. Phys.* **2002**, *203*, 2540.

[9] Y. Guo, J. van Beek, B. Zhang, M. Colussi, P. Walde, A. Zhang, M. Kröger, A. Halperin, A. D. Schlüter, *J. Am. Chem. Soc*. **2009**, *131*, 11841.

[10] L. Katsikas, M. Avramovic, R. D. Betancourt Cortes, M. Milovanovic, M. T. Kalagasidis-Krusic, I. G. Popovic, *J. Serb. Chem. Soc*. **2008**, *73*, 915.

[11] S. S. Sheiko, F. C. Sun, A. Randall, D. Shirvanyants, M. Rubinstein, H.-I. Lee, K. Matyjaszewski, *Nature* **2006**, *440*, 191.

[12] S. J. T. Van Noort, K. O. Van der Werf, B. G. De Grooth, N. F. Van Hulst, J. Greve, *Ultramicroscopy* **1997**, *69*, 117; W. Zhuang, C. Ecker, G. A. Metselaar, A. E. Rowan, R. J. M. Nolte, P. Samor, J. P. Rabe, *Macromolecules* **2005**, *38*, 473.

[13] W. W. Graessley, K. Nagasubramanian, R. Advani, D. F. Huetter, *J. Polym. Sci., Part A-2* **1968**, *6*, 1021; T. Sasaki, H. Yaguchi, *J. Polym. Sci., Part A: Polym. Chem.* **2009**, *47*, 602.

[14] B. Yamada, T. Tanaka, T. Otsu, *Eur. Polym. J.* **1989**, *25*, 117.

[15] I. M. Pinilla, M. B. Martinez, D. A. Tirrell, *Macromolecules* **1994**, *27*, 2671.

[16] J. Chiefari, J. Jeffery, R. T. A. Mayadunne, G. Moad, E. Rizzardo, S. H. Thang, *Macromolecules* **1999**, *32*, 7700.

[17] M. M. Caruso, D. A. Davis, Q. Shen, S. A. Odom, N. R. Sottos, S. R. White, J. S. Moore, *Chem. Rev.* **2009**, *109*, 5755 and refs. cit. therein.

[18] B. A. Buchholz, J. M. Zahn, M. Kenward, G. W. Slater, A. E. Barron, *Polymer* **2004**, *45*, 1223; D. McIntyre, L. J. Fetters, E. Slagowski, *Science* **1972**, *176*, 1041.

[19] A. A. Berlin, E. A. Penskaya, G. I. Volkova, *J. Polym. Sci.* **1962**, *56*, 477; V. F. Patat, W. Hogner, *Makromol. Chem.* **1964**, *75*, 85; H. H. G. Jellinek, S. Y. Fok, *Makromol. Chem.* **1967**, *104*, 18; K. B. Åbbas, R. S. Porter, *J. Polym. Sci., Polym. Chem. Ed.* **1976**, *14*, 553; K. B. Åbbas, T. Kirschner, R. S. Porter, *Eur. Polym. J.* **1978**, *14*, 361; W. G. Rand, A. K. Mukherji, *J. Polym. Sci., Polym. Lett. Ed.* **1982**, *20*, 501; V. I. Lozinsky, L. V. Domotenko, E. S. Vainerman, A. M. Mamtsis, S. V. Rogozhin, *Polym. Bull.* **1986**, *15*, 333; V. Zysman, T. Q. Nguyen, H.-H. Kausch, *J. Polym. Sci., Part B: Polym. Phys.* **1994**, *32*, 1257; S. Wang, X. Yan, J. Ding, M. Liu, R. Cheng, C. Wu, R. Qian, *J. Macromol. Sci., B: Phys.* **1997**, *36*, 187.

[20] M. V. Encina, E. Lissi, M. Sarasúa, L. Gargallo, D. Radic, *J. Polym. Sci., Polym. Lett. Ed.* **1980**, *18*, 757; K. L. Berkowski, S. L.Potisek, C. R. Hickenboth, J. S. Moore, *Macromolecules* **2005**, *38*, 8975; C. R. Hickenboth, J. S. Moore, S. R. White, N. R. Sottos, J. Baudry, S. R. Wilson, *Nature* **2007**, *446*, 423; S. L. Potisek, D. A. Davis, N. R. Sottos, S. R. White, J. S. Moore, *J. Am. Chem. Soc.* **2007**, *129*, 13808.

[21] N. Grassie, B. J. D. Torrance, *J. Polym. Sci., Part A-1: Polym. Chem.* **1968**, *6*, 3315.

[22] S. Panyukov, E. B. Zhulina, S. S. Sheiko, G. C. Randall, J. Brock, M. Rubinstein, *J. Chem. Phys. B* **2009**, *113*, 3750; S. Payukov, S. S. Sheiko, M. Rubinstein, *Phys. Rev. Lett*. **2009**, *102*, 148301; J. Paturej, L. Kuban, A. Milchev, T. A. Vilgis, *Eur. Phys. Lett.* **2012**, *97*, 58003.

[23] L. Grebikova, L. Muresan, B. Zhang, P. Maroni, A. D. Schlüter, M. Borkovec, in preparation.

Received August 15, 2012